Article

PtNPs as Scaffolds to Regulate Interenzyme Distance for Construction of Efficient Enzyme Cascade Amplification for Ultrasensitive Electrochemical Detection of MMP-2

Beibei Kou, Yaqin Chai, Yali Yuan, and Ruo Yuan

Anal. Chem., **Just Accepted Manuscript** • DOI: 10.1021/acs.analchem.7b02210 • Publication Date (Web): 20 Jul 2017

PtNPs as Scaffolds to Regulate Interenzyme Distance for Construction of Efficient Enzyme Cascade Amplification for Ultrasensitive Electrochemical Detection of MMP-2

Bei-Bei Kou, Ya-Qin Chai, Ya-Li Yuan, Ruo Yuan**

Key Laboratory of Luminescent and Real-Time Analytical Chemistry (Southwest University), Ministry of Education, College of Chemistry and Chemical Engineering, Southwest University, Chongqing 400715, PR China

*Corresponding authors at: Tel.: +86-23-68252277, fax: +86-23-68253172.

E-mail addresses: y198688@swu.edu.cn (Y. L. Yuan); yuanruo@swu.edu.cn (R. Yuan).

ABSTRACT

The high catalytic efficiency of enzyme cascade reaction mainly depends on optimal interenzyme distance regulated by the special scaffolds. In this work, the rigid PtNPs with different sizes were employed as scaffolds to regulate interenzyme distance for efficient enzyme cascade amplification to construct electrochemical biosensor for sensitive detection of matrix metalloproteinases-2 (MMP-2), which overcame the drawbacks of instable construction and sophisticated preparation induced by conventional scaffolds such as metal-organic frameworks (MOFs), DNA nanostructures. Here, cucurbit[7]uril functionalized PtNPs (CB[7]@PtNPs) were utilized to load ferrocene (Fc)-labeled horseradish peroxidase (HRP) and glucose oxidase (GOx) *via* host-guest interaction between Fc and CB[7] respectively, resulting in the formation of a stable three-dimensional netlike structure containing amounts of enzymes. Interestingly, the enzyme cascade reaction regulated by 10 nm PtNPs as scaffolds showed highly catalytic efficiency. Meanwhile, the PtNPs could also serve as catalyst to accelerate enzyme cascade reaction with further enhanced catalytic efficiency. As a result, the proposed biosensor exhibited excellent sensitivity with a wide linear range of 0.1 $pg \cdot mL^{-1}$ to 20 $ng \cdot mL^{-1}$ and a detection limit of 0.03 $pg \cdot mL^{-1}$ for MMP-2. Such strategy opened a new avenue for adopting metal nanoparticles to regulate interenzyme distance for efficient enzyme cascade amplification, thus providing a universal and easily operating method for sensitively detecting various targets such as DNA, metal ion and protein.

INTRODUCTION

The enzyme cascade amplification strategy, typically defined as a consecutive series of chemical reactions proceeding in a concurrent fashion, has been widely used in the sensitive protein detection.[1-3] In a typical case, the catalysis product generated by one type of enzyme could be used as a substrate for another coenzyme with high local concentrations, leading to prominent enhancement of catalytic efficiency compared with that of monoenzyme-catalyzed amplification.[4-6] However, many studies have demonstrated that the transport of produced substrates to adjacent coenzymes existed diffusion effect as well as inevitable subsidiary reactions, which probably reduced the concentrations of generated substrates with low catalytic efficiency.[7-9] Accordingly, the optimal interenzyme distance regulated by special scaffolds is deemed as a vital point for high-efficiency enzyme cascade amplification.[10-12]

The metal-organic frameworks (MOFs) have recently emerged as new scaffolds for encapsulating enzymes in different cavities to well regulate interenzyme distance.[13] Nevertheless, such strategy usually met the problems of insufficient access of substrates to encapsulated enzymes and low encapsulation ability, thus might be difficult to achieve high catalytic efficiency. Coincidentally, self-assembly DNA nanostructures as scaffolds can circumvent the above mentioned difficulties to some extent.[14-18] Here, the enzymes were directly assembled on DNA nanostructures, and the interenzyme distance was precisely regulated by controlling the base numbers of

DNA, providing a relatively simple fashion for constructing enzyme cascade reaction with high catalytic efficiency.[19] Despite these successes, its further application in biosensor was limited owing to the inherent defects, for example, the easy decomposition of DNA nanostructures at room temperature, and the huge consumption of DNA sequence fragments. Therefore, searching for highly efficient and stable scaffolds to solve these issues is still an urgent task.

In the present work, a novel electrochemical sensor was fabricated based on the rigid PtNPs with different sizes as scaffolds to regulate interenzyme distance for efficient enzyme cascade amplification for sensitive detection of matrix metalloproteinases-2 (MMP-2), which overcame the shortcomings of MOFs and DNA nanostructures as scaffolds. As expressed in Scheme 1, with horseradish peroxidase (HRP) and glucose oxidase (GOx) as model enzymes, cucurbit[7]uril functionalized PtNPs (CB[7]@PtNPs) were utilized to load ferrocene (Fc)-labeled horseradish peroxidase (HRP) and glucose oxidase (GOx) *via* host-guest interaction between Fc and CB[7] respectively, resulting in the formation of three-dimensional structure for immobilization of a large number of enzymes. Compared with other reported literatures,[20,21] our method offered distinctive advantages as follows: (1) PtNPs possessed the properties of rigid structure, one-pot synthesis and tunable particle size, which could be convenient for regulating interenzyme distance for efficient enzyme cascade amplification; (2) PtNPs also served as catalysts to accelerate enzyme cascade reaction, thus greatly enhancing catalytic efficiency. When the size of PtNPs was

approximated to 10 nm, the enzyme cascade reaction could show optimal catalytic efficiency, in accordance with that of previously reported works with DNA nanostructures as scaffolds.[22] Hence, the proposed biosensor exhibited excellent sensitivity with a detection limit down to subpicomolar. This strategy exploited rigid metal nanoparticles to regulate interenzyme distance for high-efficiency enzyme cascade amplification, providing a new method for the sensitive detection of protein.

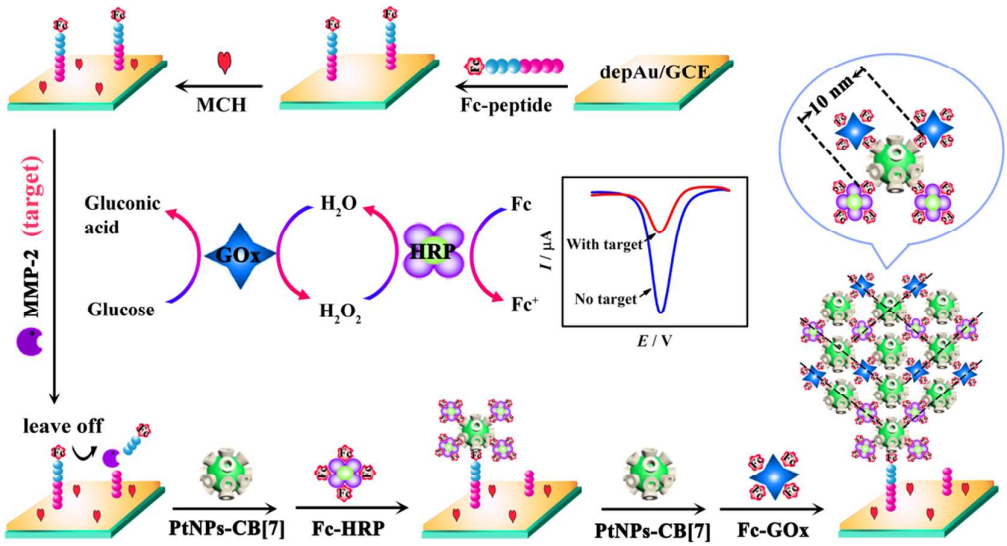

Scheme 1 Schematic illustration of PtNPs regulated highly efficient enzyme cascade amplification for electrochemical detection of MMP-2.

EXPERIMENTAL

Materials and Reagents. Cucurbit[7]uril (CB[7]), tris(2-carboxyethyl) phosphine (TCEP), glucose, ferrocene monocarboxylic acid (Fc-COOH), mercaptohexanol (MCH), N-(3-Dimethylaminopropyl)-N'-ethylcarbodiimide hydrochloride (EDC), N-Hydroxysulfosuccinimide (NHS) and carcinoembryonic

antigen (CEA) were obtained from Sigma (St. Louis, MO). Horseradish peroxidase (HRP) and glucose oxidase (GOx) were purchased from J&K Chemical Technology Co., Ltd. (Beijing, China). Matrix metalloproteinase-2 (MMP-2) and matrix metalloproteinases-7 (MMP-7) were provided by Sino Biological Inc. (Beijing, China). The peptide (NH_2-KKKPLGVRGCCC-SH) was purchased from Science Peptide Biological Technology Co., Ltd (Shanghai, China).

Apparatus. All electrochemical measurements including cyclic voltammetry (CV) and differential pulse voltammetry (DPV) were measured with CHI 660D electrochemical workstation with a conventional three-electrode system.[23] The images of various sizes of PtNPs were performed by transmission electron microscopy (TEM, H600, Hitachi, Japan).

Preparation of CB[7]@PtNPs, Fc-peptide, Fc-HRP and Fc-GOx. The 10 nm PtNPs in diameter were prepared according to the published literature with slight modification.[24] Initially, 1 mL H_2PtCl_6 aqueous solution (1%, *w/v*) was added into 40 mL of water and then heated to boiling. Afterwards, 6 mL freshly prepared sodium citrate aqueous (1%, *w/v*) was added rapidly and kept for 120 min. When the solution gradually changed from light yellow to black, indicating the formation of PtNPs. The obtained solution was treated with centrifugation, washed three times and then dispersed in 2 mL ultrapure water. After that, 200 μL CB[7] (1 mM) was mixed with the aforementioned PtNPs and shaken for 12 h. Ultimately, CB[7]@PtNPs was synthesized successfully on account of the strong multivalence interaction between

PtNPs and carbonyl groups of CB[7].[25,26] For comparison, a sequence of CB[7]@PtNPs complex with various sizes of PtNPs were synthesized.[27]

The preparation of Fc-peptide was described as follows: first, the peptide was pre-incubated with TCEP for 40 min to prevent disulfide formation between peptides. Then, 5 mg Fc-COOH was added into 1.0 mL phosphate buffered solution (PBS, pH 7.0) containing 10 mM NHS and 40 mM EDC and incubated for 1 h to activate the COOH groups. Next, 300 μL peptide solution (10 μM) was added and the reaction was kept at 4 °C overnight to obtain Fc-peptide bioconjugates. The same procedures were employed for the preparation of Fc-HRP and Fc-GOx.

Fabrication of the Electrochemical Biosensor. The cleaned glassy carbon electrode (GCE)[28] was immersed in $HAuCl_4$ (1%, *w/v*) for electrochemical deposition (depAu) under a potential of -0.2 V for 30 s. Subsequently, 15 μL Fc-peptide solution was dropped on electrode and reacted for overnight at 4 °C, followed by the incubation of 10 μL blocking agent MCH (2.0 mM) for 50 min. After that, the obtained MCH/Fc-peptide/depAu/GCE was incubated with different concentrations of MMP-2 for 50 min at 37 °C. In order to form the three-dimensional structure, 15 μL CB[7]@PtNPs, Fc-HRP, CB[7]@PtNPs and Fc-GOx (15 μM) were immobilized onto the electrode in turn and stored at room temperature for 30 min.

RESULTS AND DISCUSSIONS

Characterizations for Different Nanomaterials. The morphologies of PtNPs with four different particle sizes were characterized using TEM, and the results were

displayed in Figure 1. These images displayed the spherical structure with homogeneous distribution, and the corresponding average sizes were 4 nm, 10 nm, 20 nm and 50 nm, respectively.

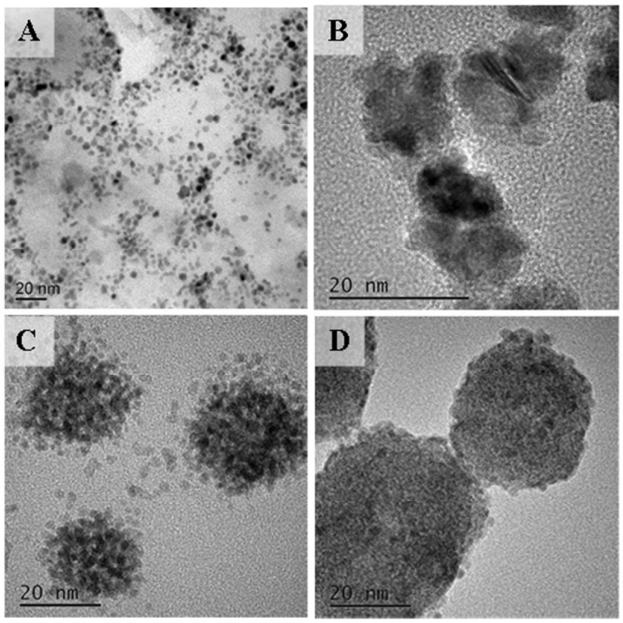

Figure 1 TEM images of PtNPs with four different particle sizes: (A) 4 nm, (B) 10 nm, (C) 20 nm, and (D) 50 nm.

Electrochemical Characterization for Different Electrode. The CV is a practical method to study interface properties for different modified electrode.[29] As displayed in Figure 2A, a well-defined redox peak was showed on the bare GCE (curve a). When AuNPs were electro-deposited onto electrode, an obvious increase in current was acquired due to the superior conductivity of depAu (curve b). When the electrode incubated with Fc-peptide solution, the current slightly increased owing to the presence of electron media Fc (curve c). However, with the introduction of

nonconductive MCH to block nonspecific binding sites, an obvious decline in current was detected (curve d). Since the target MMP-2 could specially recognize and cleave peptide with the release of Fc, the current signal further decreased (curve e) in the presence of MMP-2. Furthermore, when the electrode was successively modified with CB[7]@PtNPs, Fc-HRP, CB[7]@PtNPs and Fc-GOx to form three-dimensional netlike structure, continuous decrease in current was observed (curve f), which was attributed to the hindrance of protein and CB [7] to electron transfer.

To further confirm the high catalytic efficiency of enzyme cascade amplification, the electrochemical signals with and without 3.0 mM glucose in the detection solution were shown in Figure 2B. Before the presence of glucose, a low current signal was obtained (curve a) owing to the presence of electron media Fc. However, a significant increase in current response could be observed (curve b) with the addition of glucose. The reason may be ascribed to highly efficient enzyme cascade amplification, in which GOx catalyzed glucose to gluconic acid with the concomitant formation of H_2O_2 for accelerating the redox reaction of Fc in the assistant of HRP and PtNPs.

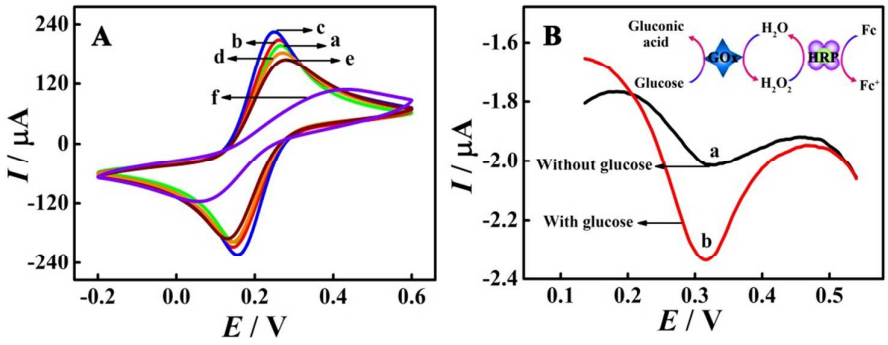

Figure 2 (A) The CVs of different electrodes in 5 mM $[Fe(CN)_6]^{3-/4-}$ solution: (a) unmodified GCE; (b) depAu/GCE; (c) Fc-peptide/depAu/GCE; (d) MCH/Fc-peptide /depAu/GCE; (e) the MCH/Fc-peptide/depAu/GCE after treated with 1 $ng \cdot mL^{-1}$ MMP-2; (f) MMP-2/MCH/Fc-peptide/depAu/GCE treated with three-dimensional netlike structure. (B) The DPV signals for constructed biosensor in the detection solution containing 2 mL of 0.1 M PBS (pH 7.4) without (a) and with (b) 3.0 mM glucose.

Optimization of Experimental Conditions. The incubation time between peptide and target MMP-2 was an important factor to obtain excellent performance for electrochemical biosensor. As seen from Figure 3A, the DPV peak current decreased with the increasing incubation time, and then remained constant after 30 min. Thus, the interaction time of 30 min was selected in this work.

The catalytic efficiency of enzyme cascade amplification largely depended on the size of PtNPs. To prove this point, the biosensor was successively modified with PtNPs in different sizes for immobilizing bi-enzyme (HRP/GOx) and the performance was evaluated by DPV experiment. As shown in Figure 3B, compared with PtNPs in 4 nm diameter, the biosensor with PtNPs in 10 nm diameter exhibited a 2-fold

increase in DPV peak current. However, increasing the particle size of PtNPs from 10 to 50 nm, a continuous decrease in current response was observed. It may arise from the fact that PtNPs with ultrasmall size would limit immobilization amount of enzymes owing to steric hindrance, while PtNPs with large size could not realize the efficient regulation of interenzyme distance, and thus led to a low catalytic efficiency. As a consequence, PtNPs in 10 nm diameter were served as the optimal size for highly efficient enzyme cascade amplification in this work.

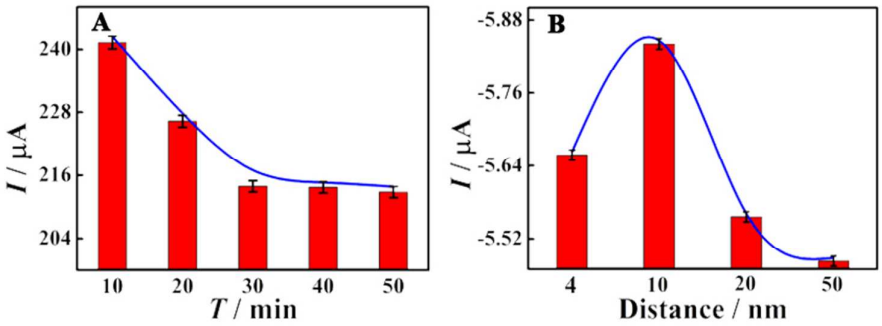

Figure 3 (A) The influence of incubation time for target MMP-2 detection, and (B) the DPV response after the proposed biosensor modified with PtNPs in different sizes from 4 nm to 50 nm. Detection buffer: 2 mL of PBS buffer (0.1 M, pH 7.4) containing 3.0 mM glucose.

Performance of Proposed Biosensor. The DPV responses for different concentrations of MMP-2 were performed under optimized conditions and the results were shown in Figure 4. The electrochemical signal decreased with increasing concentration of MMP-2 (Figure 4A). Figure 4B displayed a good linear logarithmic relationship between DPV responses and MMP-2 concentration ranging from 0.1 pg·mL^{-1} to 20 ng·mL^{-1}. The regression equation was I = 0.267 lg$c_{\text{MMP-2}}$ - 5.828 (r =

0.997) and a detection limit was estimated to be 0.03 pg·mL^{-1}. Compared with the previously reported methods for MMP-2 detection, our method showed better performance as shown in Table S1. The reason may be ascribed to highly efficient enzyme cascade amplification regulated by PtNPs as well as intrinsically excellent catalytic performance of PtNPs.

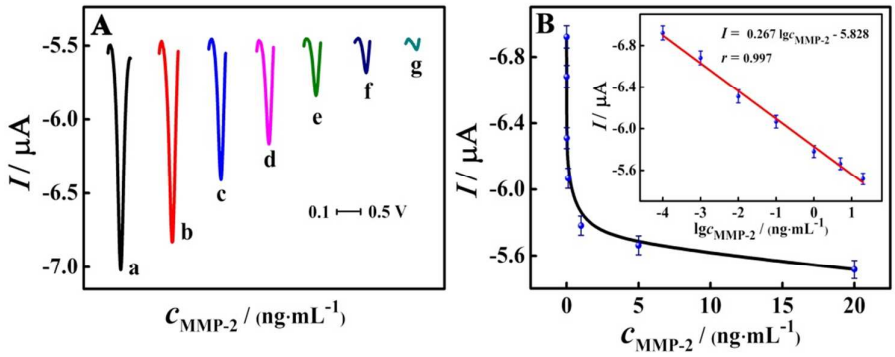

Figure 4 (A) The DPVs of MMP-2 detection with different concentrations in PBS (pH 7.4) buffer from a to g: 0.0001, 0.001, 0.01, 0.1, 1.0, 5.0, 20 ng·mL^{-1}, respectively. (B) The calibration plots for MMP-2.

Selectivity and Reproducibility of Biosensor. To evaluate the selectivity of the proposed biosensor for MMP-2 detection, several interferences such as CEA, MMP-7 and KCl were tested at the same concentrations of 10 ng·mL^{-1}. As indicated from Figure S1A, the DPV responses of biosensor that incubated with CEA, MMP-7, KCl were the same as the blank test. Furthermore, the detection signal obtained from the mixture containing above three interferences and MMP-2 had no significant change compared to that of MMP-2 (1 ng·mL^{-1}) only. These results indicated that the proposed biosensor exhibited superior selectivity for MMP-2 assay. Moreover, we

also investigated the reproducibility of proposed biosensor by using four electrodes under the same condition (Figure S1B). The relative standard deviation (RSD) was 1.07% with the same concentration of MMP-2 (1 $ng \cdot mL^{-1}$), demonstrating a remarkable reproducibility of proposed electrochemical biosensor.

Practical Application of the Biosensor. In order to assess the practical applicability of proposed biosensor, a recovery experiment was carried out by adding four various concentrations of MMP-2 into 50-fold-diluted healthy human serum. As shown in Table S2, the acceptable recoveries (ranged from 97.6% to 105%) suggested the promising potential application in clinical detection.

CONCLUSION

In summary, a novel electrochemical biosensor was fabricated for ultrasensitive detection of MMP-2 on basis of optimal interenzyme distance regulated by PtNPs for highly efficient enzyme cascade amplification. Herein, rigid PtNPs were employed as not only scaffolds to regulate interenzyme distance between HRP and GOx, but also catalyst to catalyze the reduction of H_2O_2 for signal amplification. In addition, cascaded enzymes could be flexibly fixed on PtNPs *via* host-guest interaction with the formation of stable three-dimensional netlike structure, leading to enhanced immobilization amount of enzymes with higher catalytic efficiency. The optimal interenzyme distance regulated by PtNPs can achieved highly efficient enzyme cascade amplification, holding great promise to sensitively detect various targets such as DNA, metal ion and protein.

ASSOCIATED CONTENT

Supporting Information

Comparison of this work with the previous research for MMP-2 detection, selectivity and reproducibility of biosensor, and practical application of the biosensor were supplied in Supporting Information.

ACKNOWLEDGEMENT

This work was supported by the National Natural Science Foundation (NNSF) of China (21505107, 21575116, 21675129), and the Natural Science Foundation Project of Chongqing City (cstc2016jcyjA0189).

REFERENCES

(1) Zhao, Y.; Huang, Y. C.; Zhu, H.; Zhu, Q. Q.; Xia, Y. S. *J. Am. Chem. Soc*. **2016**, *138*, 16645-16654.

(2) Filice, M.; Palomo, J. M. *ACS Catal*. **2014**, *4*, 1588-1598.

(3) Wang, L. J.; Ren, M.; Zhang, Q. Y.; Tang, B.; Zhang, C. Y. *Anal. Chem.* **2017***, 89,* 4488-4494.

(4) Hu, Y. W.; Wang, F.; Lu, C. H.; Girsh, J. L.; Golub, E.; Willner. I. *Chem. Eur. J.* **2014**, *20*, 16203-16209.

(5) Jin, L. Y.; Dong, Y. M.; Wu, X. M.; Cao, G. X.; Wang, G. L. *Anal. Chem.* **2015***, 87,* 10429-10436.

(6) Qu, R.; Shen, L. L; Qu, A. T.; Wang, R. L.; An, Y. L.; Shi, L. Q. *ACS Appl. Mater. Interfaces* **2015**, *7*, 16694-16705.

(7) Lin, J. L.; Palomec, L.; Wheeldon. I. *ACS Catal*. **2014**, *4*, 505-511.

(8) Fu, J. L.; Yang, Y. R.; Dhakal, S.; Zhao, Z.; Liu, M. H.; Zhang, T.; Walter, N. G.; Yan, H. *Nat. protocols.* **2016**, *11*, 2243-2273.

(9) Fu, J. L.; Yang, Y. R.; Johnson-Buck, A.; Liu, M. H.; Liu, Y.; Walter, N. G.; Woodbury, N. W.; Yan, H. *Nat. Nanotechnol.* **2014**, *9*, 531-536.

(10) Chado, G. R.; Stoykovich, M. P.; Kaar, J. L. *ACS Catal*. **2016**, *6*, 5161-5169.

(11) Sun, J. Y.; Ge, J. C.; Liu, W. M.; Lan, M. H.; Zhang, H. Y.; Wang, P. F.; Wang, Y. M.; Niu, Z. W. *Nanoscale* **2014**, *6*, 255-262.

(12) You, M. X.; Wang, R. W.; Zhang, X. B.; Chen, Y.; Wang, K. L.; Peng, L.; Tan, W. H. *ACS Nano* **2011**, *5*, 10090-10095.

(13) Lian, X. Z.; Chen, Y. P.; Liu, T. F.; Zhou, H. C. *Chem. Sci*. **2016**, *7*, 6969-6973.

(14) Timm, C.; Niemeyer, C. M. *Angew. Chem. Int. Ed*. **2015**, *54*, 6745-6750.

(15) Xin, L.; Zhou, C.; Yang, Z. Q.; Liu, D. S. *Small* **2013**, *9*, 3088-3091.

(16) Wang, F.; Lu, C. H.; Willner, I. *Chem. Rev*. **2014**, *114*, 2881-2941.

(17) Fu, Y. M.; Zeng, D. D.; Chao, J.; Jin, Y. Q.; Zhang, Z.; Liu, H. J.; Li, D.; Ma, H. W.; Huang, Q.; Gothelf, K. V.; Fan, C. H. *J. Am. Chem. Soc.* **2013**, *135*, 696-702.

(18) Liu, M. H.; Fu, J. L.; Hejesen, C.; Yang, Y. H.; Woodbury, N. W.; Gothelf, K.; Liu, Y.; Yan, H. *Nat. Commun.* **2013**, *4*.

(19) Fu, J. L.; Liu, M. H.; Liu, Y.; Woodbury, N. W.; Yan, H. *J. Am. Chem. Soc.* **2012**, *134*, 5516-5519.

(20) Xiang, B. B.; He, K. Y.; Zhu, R.; Liu, Z. L; Zeng, S.; Huang, Y.; Nie, Z.; Yao, S. Z. *ACS Appl. Mater. Interfaces* **2016**, *8*, 22801-22807.

(21) Lu, S. S.; Hu, T.; Wang, S.; Sun, J.; Yang, X. R. *ACS Appl. Mater. Interfaces* **2017**, *9*, 167-175.

(22) Ngo, T. A.; Nakata, E.; Saimura, M.; Morii, T. *J. Am. Chem. Soc.* **2016**, *138*, 3012-3021.

(23) Yang, Z. H.; Zhuo, Y.; Yuan, R.; Chai, Y. Q. *Anal. Chem.* **2016**, *88*, 5189-5196.

(24) Wu, X. Y.; Chai, Y. Q.; Zhang, P.; Yuan, R. *ACS Appl. Mater. Interfaces* **2015**, *7*, 713-720.

(25) Husken, N.; Taylor, R. W.; Zigah, D.; Taveau, J. C.; Lambert, O.; Scherman, O. A.; Baumberg, J. J.; Kuhn, A. *Nano Lett.* **2013**, *13*, 6016-6022.

(26) Taylor, R. W.; Lee, T. C.; Scherman, O. A.; Esteban, R.; Aizpurua, J.; Huang, F. M.; Baumberg, J. J.; Mahajan, S. *ACS Nano* **2011**, *5*, 3878-3887.

(27) Bigall, N. C.; Hartling, T.; Klose, M.; Simon, P.; Eng, L. M.; Eychmuller, A. *Nano Lett.* 2008, *8*, 4588-4592.

(28) Zhang, P.; Li, Z. Y.; Wang, H. J.; Zhuo, Y.; Yuan, R.; Chai, Y. Q. *Nanoscale* **2017**, *9*, 2310-2316.

(29) Wu, H.; Fan, S. H.; Jin, X. Y.; Zhang, H.; Chen, H.; Dai, Z.; Zou, X. Y. *Anal. Chem*. **2014**, *86*, 6285-6290.

For TOC only